How to cite: *Angew. Chem. Int. Ed.* **2020**, *59*, 17548–17555
International Edition: doi.org/10.1002/anie.202005004
German Edition: doi.org/10.1002/ange.202005004

Cancer Metastasis

# Targeted Degradation of Transcription Coactivator SRC-1 through the N-Degron Pathway

*Yeongju Lee, Jiwon Heo, Hoibin Jeong, Kyung Tae Hong, Do Hoon Kwon, Min Hyeon Shin, Misook Oh, Ganesh A. Sable, G-One Ahn,* Jun-Seok Lee,* Hyun Kyu Song,* and Hyun-Suk Lim**

***Abstract:*** *Aberrantly elevated steroid receptor coactivator-1 (SRC-1) expression and activity are strongly correlated with cancer progression and metastasis. Here we report, for the first time, the development of a proteolysis targeting chimera (PROTAC) that is composed of a selective SRC-1 binder linked to a specific ligand for UBR box, a unique class of E3 ligases recognizing N-degrons. We showed that the bifunctional molecule efficiently and selectively induced the degradation of SRC-1 in cells through the N-degron pathway. Importantly, given the ubiquitous expression of the UBR protein in most cells, PROTACs targeting the UBR box could degrade a protein of interest regardless of cell types. We also showed that the SRC-1 degrader significantly suppressed cancer cell invasion and migration in vitro and in vivo. Together, these results demonstrate that the SRC-1 degrader can be an invaluable chemical tool in the studies of SRC-1 functions. Moreover, our findings suggest PROTACs based on the N-degron pathway as a widely useful strategy to degrade disease-relevant proteins.*

## Introduction

Steroid receptor coactivator-1 (SRC-1, also known as NCOA-1) is the first identified transcription coactivator that promotes the transcriptional activities of various transcription factors (TFs), such as the estrogen receptor α, the progesterone receptor, etc.[1] SRC-1 belongs to the p160 SRC family that includes other homologous members, SRC-2 (NCOA-2) and SRC-3 (NCOA-3).[2–4] It contains four domains including the activation domain (AD) 3 in N-terminus, a nuclear receptor interaction domain, and AD1 and AD2 in C-terminus. As a coactivator, SRC-1 not only interacts with TFs, but also recruits various proteins to assemble multi-protein complexes.[5–8] As a consequence, SRC-1 drives chromatin remodeling and transcriptional activation and plays a critical role in regulating diverse biological processes, such as cell cycle, energy metabolism, and inflammation.[9] At normal physiological conditions, only limited concentrations of cellular SRC-1 are present, indicating that abnormally activated SRC-1 is linked to various human diseases such as cancer. Indeed, aberrantly elevated SRC-1 expression and activity are observed in many types of cancers and strongly implicated in cancer metastasis, recurrence, drug resistance, and poor prognosis.[10,11] Therefore, SRC-1 has been recognized as an oncogenic protein, and thus inhibition of SRC-1 represents a valid therapeutic strategy for the treatment of various cancers. However, the development of molecules modulating transcriptional activity has proven to be very challenging because it generally requires to target protein-protein interactions (PPIs).[12–14] Nonetheless, several SRC-1 inhibitors have been developed to date.[15–18] For instance, a small molecule targeting both SRC-1 and SRC-3 recently reported by O'Malley and co-workers exhibited potent in vitro and in vivo activities.[17] However, they lack the selectivity to SRC-1, and their mode of action remains unclear.

Herein, we describe, for the first time, the discovery of PROTAC-based molecules that selectively inhibit SRC-1. PROTACs are heterodimeric molecules that bind to a target protein of interest and an E3 ubiquitin ligase simultaneously.[19–22] These chimeric molecules are able to recruit the target protein to the E3 ligase, otherwise they do not interact at all. As a result, the target protein is polyubiquitinated and subsequently degraded by the 26S proteasome. Given its ability to effectively eliminate a target protein (e.g., disease-causing proteins) in the cells, PROTACs technology is emerging as a novel therapeutic modality in drug discovery. Despite its utility as a tool to identify therapeutic candidates and chemical probes, current PROTACs have limitations. For example, while there are over 600 E3 ubiquitin ligases, only a few, such as cereblon (CRBN) and Von Hippel-Lindau tumor suppressor (VHL), are mostly used in PROTAC design.[20–29] When targeting tissues or cells that do not express such E3 ligases sufficiently, it is impossible to create

[*] Y. Lee, M. H. Shin, M. Oh, G. A. Sable, H.-S. Lim
Department of Chemistry and Division of Advanced Materials Science, Pohang University of Science and Technology (POSTECH)
77 Cheongam-Ro, Nam-Gu, Pohang 37673 (South Korea)
E-mail: hslim@postech.ac.kr
J. Heo, D. H. Kwon, H. K. Song
School of Life Sciences and Biotechnology, Korea University
145 Anam-ro, Seongbuk-gu, Seoul 02841 (South Korea)
E-mail: hksong@korea.ac.kr
H. Jeong, G-O. Ahn
Research Institute for Veterinary Science and College of Veterinary Medicine, Seoul National University
1 Gwanak-ro, Gwanak-gu, Seoul 08826 (South Korea)
E-mail: goneahn@snu.ac.kr
K. T. Hong, J.-S. Lee
Molecular Recognition Research Center, Korea Institute of Science and Technology (KIST)
5. Hwarang-ro, 14-gil, Seongbuk-gu, Seoul 02792 (South Korea)
E-mail: junseoklee@chembiol.re.kr
Supporting information and the ORCID identification number(s) for the author(s) of this article can be found under: https://doi.org/10.1002/anie.202005004.

  

a PROTAC molecule. To circumvent such obstacles, here we developed novel PROTAC molecules capable of selectively degrading SRC-1 through the N-degron pathway (also known as the N-end rule pathway) (Figure 1a).[30] The N-degron pathway is a proteolytic system in which the N-terminal amino acids of short-lived proteins are recognized by the

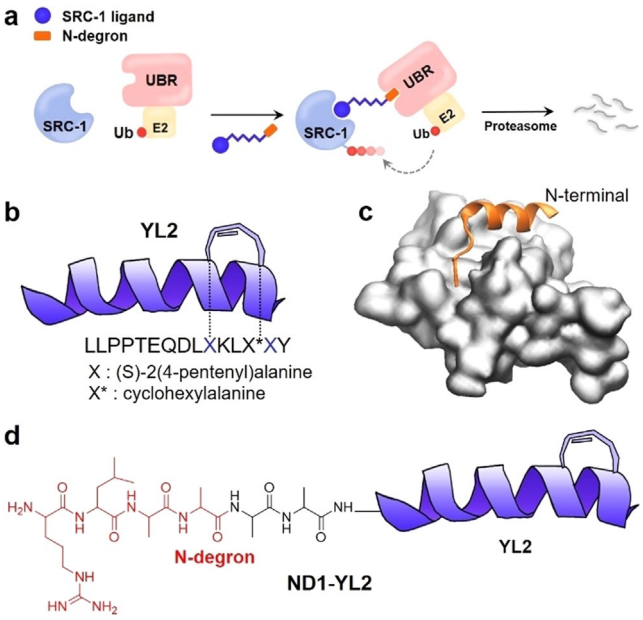


***Figure 1.*** a) SRC-1 degradation by a PROTAC through the N-degron pathway. b) Structure of a stapled peptide **YL2** as a specific SRC-1 ligand. c) Co-crystal structure of **YL2** with the PAS-B domain of SRC-1 (PDB 5Y7W). d) Structure of a bifunctional SRC-1 degrader, **ND1-YL2**.

UBR proteins, an E3 ubiquitin ligase family containing UBR box, for ubiquitination and subsequent degradation of the substrate proteins. Therefore, the N-degron pathway determines the fate of target proteins in the cells depending on the identity of N-terminal amino acids of proteins.[31–34] Given that the UBR proteins are ubiquitously expressed in most cells, PROTACs consisting of a ligand for the UBR box could degrade a protein of interest regardless of cell types.[35,36] Here, we report the development of a first-in-class SRC-1 selective degrader (**ND1-YL2**) composed of a selective SRC-1 binder linked to a specific ligand for the UBR protein. Furthermore, we have shown that targeted degradation of SRC-1 by **ND1-YL2** significantly suppresses cancer invasion and migration in vitro and in vivo. Taken together, our study suggests that the degradation of SRC-1 through the N-degron pathway is a promising anticancer therapeutic strategy, particularly for preventing cancer metastasis.

## Results and Discussion

We previously discovered a cell-permeable, stapled peptide **YL2** that mimics an LXXLL helical peptide fragment (where L is leucine and X is any amino acid) in the transactivation domain of signal transducer and activator of transcription 6 (STAT-6) (Figure 1b).[37] STAT-6 is a TF playing a pivotal role in regulating inflammatory signaling pathways in response to interleukin (IL)-4 and IL-13.[38–42] For the transcriptional activation of STAT-6, the recruitment of coactivators such as SRC-1 is required.[43] Given that STAT-6 directly interacts with the PAS-B domain (a part of the AD3 domain) of SRC-1 through the LXXLL motif, **YL2** as an LXXLL helix mimetic was able to potently disrupt the TF/coactivator interaction by binding to the PAS-B domain.[44] As a result, **YL2** suppresses STAT-6-mediated transcription and represents a novel class of therapeutic candidates for the treatment of human diseases including inflammatory allergic diseases. It is noteworthy that **YL2** is specific for SRC-1 because it has a peptide sequence derived from the PAS-B domain of STAT-6, which is known to bind specifically to SRC-1, but not the other SRC family members.[43] With a potent and selective ligand for SRC-1, we hypothesized that the conjugation of **YL2** to an E3 ligase ligand would provide a novel PROTAC molecule that brings SRC-1 and the E3 ubiquitin ligase into close proximity, thereby facilitating SRC-1 ubiquitination and degradation in the cells. Hence, inducing SRC-1 degradation would lead to suppression of SRC-1-mediated transcription and cancer metastasis and thus represents a promising anticancer strategy.

To develop such SRC-1 degraders, we chose a tetrapeptide RLAA as a UBR binder that is an N-degron fragment and binds to the UBR box (from yeast Ubr1) with a reasonably good binding affinity ($K_D = 4.2\ \mu M$).[45] Based on our previous X-ray and biochemical studies,[45] the N-terminal arginine and hydrophobic side chain of leucine were found to be critical for the interaction of the tetrapeptide with the acidic and hydrophobic clefts on the UBR domain surface. Importantly, the tetrapeptide is a natural substrate sequence of UBR ubiquitin ligase and should be inherently specific. Taken together, the UBR binding peptide would be suitable for the design of bifunctional SRC-1 degraders. The examination of the crystal structure of **YL2** in complex with the PAS-B domain of SRC-1 revealed that the N-terminal of **YL2** is solvent-exposed and could be a suitable position for conjugating a linker and the N-degron peptide (Figure 1c).[37] Based on this analysis, we designed a series of bifunctional peptides (**ND1-YL2** through **ND6-YL2**) consisting of **YL2** and RLAA, which are connected by various linkers such as Ala-Ala, aminobutanoic acid (Abu), aminohexanoic acid (Ahx), mono(ethylene glycol), di(ethylene glycol), and tri(ethylene glycol) (Figure 1d and Table S1). Peptide sequences of these chimeric molecules were prepared by standard Fmoc-based solid-phase peptide synthesis (Scheme S1 in the Supporting Information). Then, macrocyclization for the synthesis of all-hydrocarbon stapled peptides was achieved by a ring-closing olefin metathesis reaction to give bifunctional peptides. Final products were cleaved from solid-phase resin and purified by reverse-phase HPLC (Figure S1).

To evaluate the ability of the bifunctional peptides to degrade SRC-1 in the cells, human triple-negative breast cancer (TNBC) MDA-MB-231 cells were treated with DMSO or various concentrations of the synthesized peptides. Cellular levels of SRC-1 were measured by immunoblotting. Gratifyingly, robust SRC-1 degradation was observed upon

  

treatment of some of the bivalent peptides. Among the tested compounds, **ND1-YL2** having two alanines as a linker exhibited the most potent activity in reducing cellular SRC-1 levels in a dose-dependent fashion with the $DC_{50}$ of ≈ 10 μM, while the other peptides had less or no degradation activity (Figure 2a and Figure S2). Thus, we selected **ND1-YL2** as the best compound and used it for further studies.

As expected, the degradation of SRC-1 by **ND1-YL2** was blocked by co-treatment of MG-132, a well-known proteasome inhibitor (Figure 2a), confirming that **ND1-YL2** induced SRC-1 degradation through the proteasome-mediated pathway. To assess the time-dependent degradation of SRC-1, MDA-MB-231 cells were exposed to **ND1-YL2** (20 μM), and cellular levels of SRC-1 were measured by the Western blot over time. As shown in Figure 2b, SRC-1 degradation was evident at 8 h after treating **ND1-YL2** and remained through 24 h without detectable recovery of SRC-1 levels. We then monitored SRC-1 abundance over time after washing out **ND1-YL2** and found that SRC-1 levels were recovered within 12 h after the removal of **ND1-YL2** (Figure 2c), suggesting that the degradation of SRC-1 by **ND1-YL2** is reversible, in contrast to conventional genetic methods.

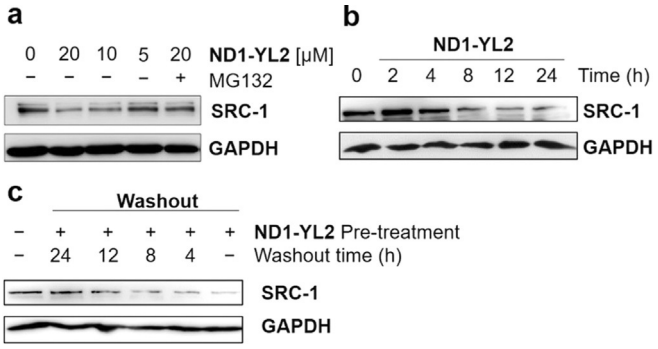


***Figure 2.*** a) Western blot analysis of SRC-1 levels in MDA-MB-231 cells after treatment of **ND1-YL2** or MG132 (5 μM) for 12 h. b) Western blot analysis of SRC-1 levels in MDA-MB-231 cells after treatment of **ND1-YL2** (20 μM) with different treatment time. c) Western blot analysis of SRC-1 levels in MDA-MB-231 cells time-dependently after **ND1-YL2** (20 μM) washout.

In order to achieve effective degradation of SRC-1, it is essential for **ND1-YL2** to render the formation of a cooperative ternary complex in which the chimeric peptide **ND1-YL2** potently binds to both SRC-1 and UBR proteins simultaneously. First, we measured circular dichroism (CD) spectra to explore whether **ND1-YL2** retained the helical propensity, which is important for its binding affinity to SRC-1 recognizing LXXLL-containing helical motifs. **ND1-YL2** was found to display similar CD spectra to that of **YL2** (Figure S3), implying that the conjugation of the linker and RLAA tetrapeptide did not affect the helicity of the original stapled peptide **YL2** (Figure S3). We then performed competitive fluorescence polarization (FP) assays to assess the binding affinities of **ND1-YL2** to the target proteins (Figure 3a). As depicted in Figure 3a, **ND1-YL2** bound the PAS-B domain of SRC-1 with the $K_i$ value of 320 nM, which is comparable with that of the original stapled peptide **YL2** ($K_i$ = 140 nM). In addition, **ND1-YL2** was tested for its ability

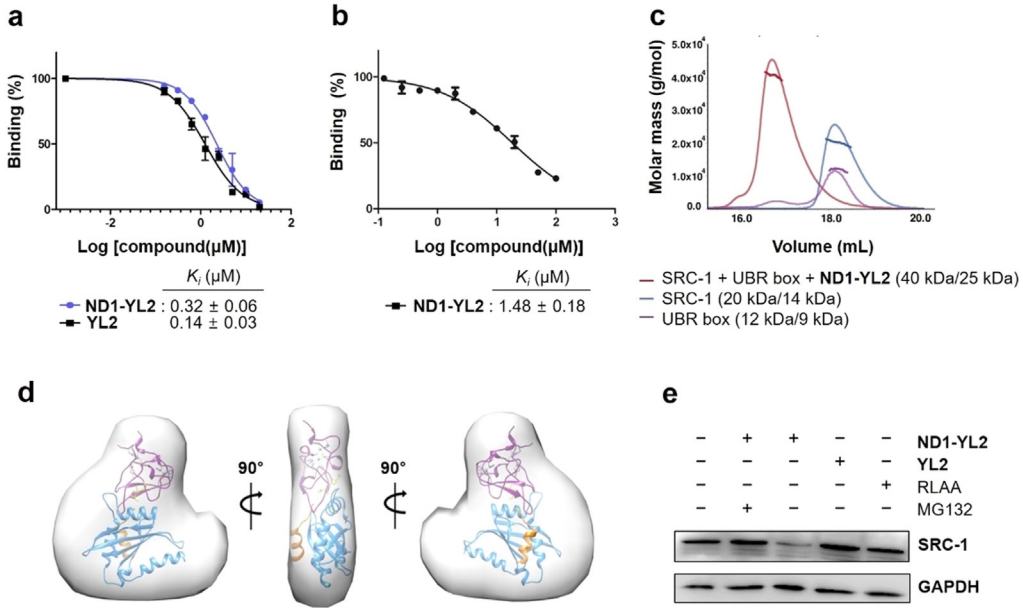


***Figure 3.*** Ternary complex formation of SRC-1—UBR box—**ND1-YL2**. a) Inhibition curves of **ND1-YL2** or **YL2** for fluorescently-labeled STAT-6 peptide binding to SRC-1 as determined by FP assays. Error bars indicate standard deviation from three independent experiments. b) Inhibition curves of **ND1-YL2** for fluorescently-labeled RLAA peptide binding to UBR-1 as determined by FP assays. Error bars indicate standard deviation from three independent experiments. c) SEC-MALS analysis of the ternary complex. Experimental molecular masses of SRC-1 (blue), UBR box (purple), and SRC-1—UBR box N**D1-YL2** complex (red) are 20, 12 and 40 kDa, respectively (The calculated values are 14, 9 and 25 kDa, respectively). d) Solution SAXS structure of SRC-1—UBR box—**ND1-YL2** ternary complex with high resolution structures of individual models. Crystal structure of SRC-1 with **YL2** (PDB ID: 5Y7W) is shown in blue (SRC-1) and orange (**YL2**), and UBR box with RLLA peptide (PDB ID: 3NIN) is shown in purple (UBR box) and yellow (RL peptide), respectively. e) Western blot analysis of SRC-1 levels in MDA-MB-231 cells after treatment of **ND1-YL2** (20 μM), **YL2** (20 μM), or RLAA peptide (20 μM).

  

to displace a fluorescent-labeled RLAA peptide from UBR box using FP assays (Figure 3b). It exhibited approximately 3-fold improved affinity against UBR box ($K_i = 1.48\ \mu M$) compared to RLAA tetrapeptide ($K_D = 4.2\ \mu M$) presumably because of the additional contact with the UBR box conferred by the linker.

The next step was to confirm whether **ND1-YL2** was capable of forming the ternary complex. When we performed the size-exclusion chromatography (SEC), both SRC-1 and UBR box protein co-migrated in solution in the presence of **ND1-YL2**, and the results of multi angle light scattering coupled with SEC (SEC-MALS) clearly showed the ternary complex formation of SRC-1/**ND1-YL2**/UBR box (experimental molecular mass of 40 kDa). Individual molecules, SRC-1 and UBR box, gave molecular masses of 20 and 12 kDa, respectively (Figure 3c). This result suggested that the SRC-1/**ND1-YL2**/UBR box formed the 1:1:1 ternary complex. To further probe this, the small-angle X-ray scattering (SAXS) was also performed, and high resolution models of SRC-1 with **YL2** (PDB ID: 5Y7W) and UBR box with RLGES (PDB ID: 3NIN) were fitted into the molecular envelope of the ternary SRC-1/**ND1-YL2**/UBR box complex. As depicted in Figure 3d, **ND1-YL2** bridges SRC-1 and UBR box, making them in close proximity.

To further verify if SRC-1 degradation was resulted from the formation of a ternary complex in the cells, cells were treated with stapled peptide (**YL2**) alone or UBR binding tetrapeptide (RLAA), and cellular levels of SRC-1 were monitored by immunoblot (Figure 3e). Not surprisingly, either **YL2** or RLAA tetrapeptide itself did not affect SRC-1 levels. Moreover, the degradation of SRC-1 by **ND1-YL2** was abolished by adding an excess amount of either **YL2** or RLAA (Figure S5), confirming that **ND1-YL2** competes with **YL2** and RLAA to bind SRC1 and UBR, respectively. Consistent with the various biochemical experiments described above (Figure 3a–d), this finding demonstrated that the formation of close proximity between SRC-1 and UBR box by **ND1-YL2** is crucial for SRC-1 degradation. We sought to compare the efficacy of **ND1-YL2** with that of an SRC-1 degrader based on the current PROTAC approach. To this end, we synthesized a series of chimeric PROTAC molecules consisting of **YL2** linked to pomalidomide, a potent small-molecule ligand for CRBN ($K_i = 156$ nM), which is one of the most commonly used E3 ligase ligands in PROTAC design (Scheme S2).[46] We then tested the cellular activity of the synthesized pomalidomide-based bifunctional molecules connected by different linkers including diethylene glycol, triethylene glycol, or tetraethylene glycol in MDA-MB-231 cells. Among them, **CL1-YL2** containing a diethylene glycol linker (Figure 4a) was the most effective in reducing SRC-1 levels (Figure 4b and Figure S7). Intriguingly, **CL1-YL2** displayed similar activity to **ND1-YL2** in inducing SRC-1 degradation, even though **ND1-YL2** has much less potent binding affinity to its target E3 ligase as compared with **CL1-YL2** (about 10-fold difference in their binding activities). This might be likely due to the catalytic nature of **ND1-YL2** in protein degradation through the N-degron pathway, along with high expression levels of UBR proteins in cells. However, we cannot rule out the possibility that similar levels of cellular activities of **ND1-YL2** and **CL1-YL2** may be because their linker lengths are not optimized. We speculated that **ND1-YL2** would be able to degrade cellular SRC-1 regardless of cell types because UBR proteins are widely expressed throughout different cells,[35] while most current PROTACs cannot be used in cells or tissues that do not express their target E3 ligase. To examine this, increasing concentrations of **ND1-YL2** or **CL1-YL2** were treated to human colon carcinoma Colo205 cells that express very low levels of CRBN. As expected, **ND1-YL2** indeed induced significant downregulation of SRC-1 in a dose-dependent manner whereas **CL1-YL2** had no effect (Figure 4c). This highlights that PROTACs based on the N-degron pathway would be highly useful and generally applicable tools in targeted protein degradation in various diseases.

We then asked whether **ND1-YL2** could selectively target SRC-1 over the other SRC family members. Given the structural similarity among the SRC members, **ND1-YL2** may also bind to and degrade the other members such as SRC-3.

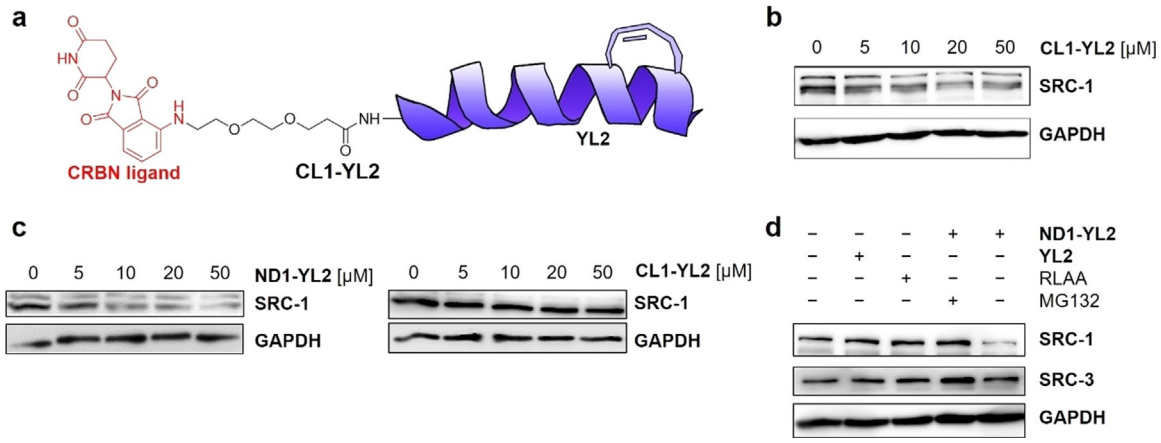


***Figure 4.*** a) Structure of **CL1-YL2**. b) Western blot analysis of SRC-1 levels in MDA-MB-231 cells after treatment of **CL1-YL2** for 12 h. c) Western blot analysis of SRC-1 levels in Colo205 cells, which have low expression level of CRBN, after treatment of varying concentrations of **ND1-YL2** or **CL1-YL2**. d) Western blot analysis of SRC-1 and SRC-3 levels in MDA-MB-231 cells after treatment of **ND1-YL2** (20 μM), **YL2** (20 μM), RLAA peptide (20 μM), or MG132 (5 μM).

  

To test this, we treated TNBC MDA-MB-231 cells with **ND1-YL2** and evaluated cellular levels of SRC-3 by Western blotting (Figure 4d). Notably, no SRC-3 degradation was observed, underscoring that **ND1-YL2** is a selective SRC-1 degrader. This result was consistent with the fact that STAT-6 interacts with SRC-1, but not SRC-3.[43] That is, given that the stapled peptide part of **ND1-YL2** was derived from the SRC-1 binding peptide motif of STAT-6, the resulting chimeric peptide **ND1-YL2** can induce selective degradation of SRC-1 by specifically binding to SRC-1. Alternatively, however, the selectivity of **ND1-YL2** could potentially be attributed to the consequence of stable ternary complex formation with SRC-1, but not SRC-3.

With a potent SRC-1 degrader in hand, we explored its pharmacological effects on SRC-1 dependent signaling. SRC-1 is overexpressed in various cancers and plays a pivotal role in elevating cell migration and invasion by regulating the expression of associated genes.[10,11] Hence, **ND1-YL2** as an SRC-1 degrader would repress the expression of genes stimulated by SRC-1 such as *colony stimulating factor-1* (*CSF-1*), a gene that codes for a cytokine CSF-1 causing cell differentiation and migration. To examine this, TNBC MDA-MB-231 cells were treated with DMSO and varying concentrations of **ND1-YL2**, **YL2**, or N-degron tetrapeptide for 12 h, and the mRNA levels of *CSF-1*, which was normalized to *18S* levels, were monitored by quantitative real-time polymerase chain reaction (RT-qPCR). Indeed, **ND1-YL2** downregulated *CSF-1* expression while **YL2** and RLAA peptide had no significant effect (Figure 5a). Additionally, we tested the effect of **ND1-YL2** on the expression of *E-cadherin*, a tumor suppressor gene playing an important role in cell-cell adhesion. Since SRC-1 protein is known to inhibit *E-cadherin* expression, **ND1-YL2** would upregulate *E-cadherin* by depleting SRC-1. As anticipated, the treatment of **ND1-YL2** resulted in a dose-dependent increase of *E-cadherin* whereas the control compounds (**YL2** and RLAA) were inactive (Figure 5b). These results are consistent with the previous studies showing that siRNA-induced SRC-1 knockdown induces downregulation of *CSF-1* and upregulation of *E-cadherin*.[10,47]

Since SRC-1 degradation effectively affects SRC-1-mediated transcription (Figure 5a and b), **ND1-YL2** would exert a suppressive effect on the downstream signaling pathways such as increased cancer cell migration and invasion.[3,17] To test this, we first performed a gap-closure migration assay using invasive TNBC MDA-MB-231 cell lines. Cells were grown to confluence in culture-insert wells, and the insert was removed to create a wound gap. Cells were then allowed to migrate for 72 h after treating DMSO, **YL2**, RLAA peptide, or **ND1-YL2**. The images of cells filling the gap were analyzed to quantify the cell migration. As depicted in Figure 5c and d, **ND1-YL2** remarkably blocked wound closure by $>80\%$, while no significant gap closure was observed in cells treated with **YL2** or RLAA peptide. The results validated that SRC-1 degradation caused by **ND1-YL2** inhibited SRC-1-mediated cell migration. Next, we carried out a transwell invasion assay to examine the effect of **ND1-YL2** on cell invasion. We treated MDA-MB-231 cells with varying concentrations of **ND1-YL2**, the N-degron (20 μM), or **YL2** (20 μM). After 24 h, invading cells were visualized and quantified with immunofluorescent microscopy. In consistent with the cell migration experiment (Figure 5c and 5d), the treatment of **ND1-YL2** resulted in a decrease in cell invasion in a dose-dependent manner, while no significant effect was observed for **YL2** or RLAA peptide (Figure 5e and f). Note that the original stapled peptide **YL2** specifically disrupts the SRC-1/STAT-6 interaction without affecting the interaction of SRC-1 with cancer-associated TFs, and therefore **YL2** alone was supposed to have no effect on cancer cell invasion and migration. Inhibitory activities of **ND1-YL2** on cell migration and invasion are in a good agreement with the previous SRC-1 knockdown experiments.[10,48] The impaired cell migration and invasion might be due to the inhibitory effect of **ND1-YL2** on cell growth. To rule out this possibility, MTT cell viability assays were performed. Consistent with the previous result observed in siRNA-induced SRC-1 knockdown,[49] SRC-1 degradation by **ND1-YL2** had no significant effect on the viability of various cell lines (Figure S8). Taken together, our data suggest that the chemical knockdown of SRC-1 by **ND1-YL2** would be an effective means to suppress cancer cell migration and invasion. Finally, we asked whether **ND1-YL2** could suppress cancer metastasis in vivo. **ND1-YL2** or vehicle (DMSO) treated TNBC MDA-MB-231 cells, which express a red fluorescent protein (RFP), were injected to BALD/c-nude mice ($n=10$ for vehicle or $n=11$ for **ND1-YL2**). After 2 weeks, treated mice were sacrificed, and lung metastasis of MDA-MB-231-RFP cells was evaluated and quantified using fluorescence-activated cell sorting (FACS) analysis. Upon treatment of **ND1-YL2**, invaded MDA-MB-231-RFP cells were reduced remarkably by 40%, as compared with the vehicle sample (Figure 6a and Figure S9). To visualize lung metastasis, we prepared the lung section and stained with Haemotoxylin and Eosin (H&E) staining. Metastatic tumors were only found in lung sections from the mice which were injected with DMSO treated MDA-MB-231 cells, while no metastatic tumors were found in the sample treated with **ND1-YL2** (Figure 6b). These results underscore that SRC-1 degradation by **ND1-YL2** efficiently suppresses the metastasis of breast cancer cells in vivo.

## Conclusion

In summary, we have developed the first PROTAC molecule (**ND1-YL2**) that induces the selective degradation of SRC-1 through the N-degron pathway. **ND1-YL2** as an SRC-1 degrader was found to significantly impair SRC-1-mediated transcriptional activity, thereby leading to the suppression of cancer cell invasion and migration in vitro and in vivo. Our results suggest that pharmacological degradation of SRC-1 would be a promising anticancer strategy. Furthermore, this work also demonstrates that our strategy to generate cell-permeable peptide PROTACs would be broadly applicable to target undruggable proteins including intracellular PPIs that are not readily tractable by traditional small-molecule based approaches. It is noteworthy that this type of PROTACs consisting of peptide ligands targeting PPIs might be relatively free from concerns about

  

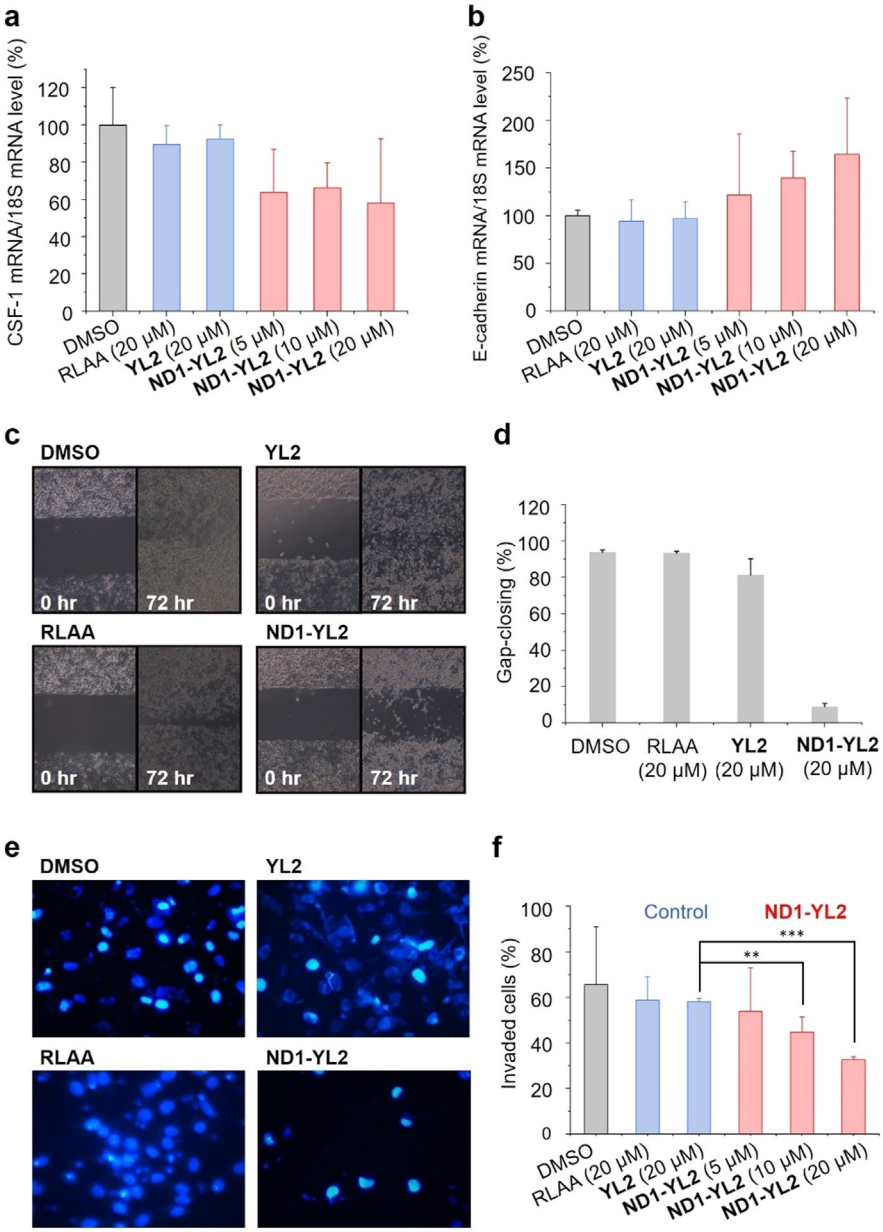


***Figure 5.*** Cellular activity of **ND1-YL2**. For RT-qPCR experiments, mRNA levels of *CSF-1* (a) and *E-cadherin* (b) were measured in MDA-MB-231 cells after treating **YL2**, RLAA peptide, or **ND1-YL2**. c) Gap-closure migration assay. The images were captured in MDA-MB-231 cells after 72 h treatment of **YL2** (20 μM), RLAA peptide (20 μM), or **ND1-YL2** (20 μM). d) The graphical data represents the percentage of gap-closed area in MDA-MB-231 cells. e) Transwell cell invasion assay. The images were captured in MDA-MB-231 cells after 24 h treatment of DMSO, **YL2** (20 μM), RLAA peptide (20 μM),or **ND1-YL2** (20 μM). f) Transwell cell invasion assay. The graphical data represents the percentage of invaded cells in MDA-MB-231 cells. Error bars indicate the standard deviation from three independent experiments. ** $P<0.01$ and *** $P<0.001$, as determined by a two-tailed Student t-test.

drug resistance compared to small molecule PROTACs,[50,51] because they are composed of endogenous peptide ligands. On the other hand, one advantage of PROTACs is that it is possible to afford a pharmacologically active PROTAC compound with desired functions even though an original ligand for protein of interest does not possess the desired activity. In this study, we show that the SRC-1 degrader capable of suppressing cell invasion and migration can be generated from an SRC-1 ligand without such activities. Collectively, we believe that **ND1-YL2** will serve as an invaluable chemical tool to probe SRC-1 functions and could be further developed as a new class of therapeutic candidates. We anticipate that PROTACs based on the N-degron pathway will be an attractive and widely applicable strategy to degrade disease-relevant proteins.

  

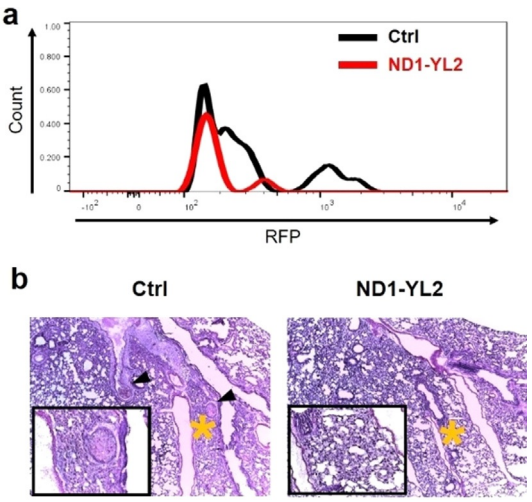


***Figure 6.*** In vivo mice studies. a) Representative FACS histograms of single-cell suspensions prepared from the lung of mice. An overlayed image of Ctrl and **ND1-YL2**. b) Representative images of metastatic tumor cells in the lung. Black arrows indicate the metastatic tumor cells in the lung.

## *Acknowledgements*

We thank Prof. John A. Robinson (University of Zürich) for the plasmid expressing SRC-1 and Prof. Won Jong Kim (POSTECH) for providing access to a CD spectrometer and an RT-PCR system. This work was supported by the National Research Foundation of Korea (NRF-2017R1A2B3004941, NRF-2018R1A4a1024713, and NRF-2019M3e5d4065251).

## *Conflict of interest*

The authors declare no conflict of interest.

**Keywords:** cancer metastasis · proteolysis-targeting chimers (PROTACs) · SRC-1 transcriptional co-activator · stapled peptide · the N-degron pathway

[1] S. A. Oñate, S. Y. Tsai, M.-J. Tsai, B. W. O'Malley, *Science* **1995**, *270*, 1354 – 1357.
[2] J. Xu, Q. Li, *Mol. Endocrinol.* **2003**, *17*, 1681 – 1692.
[3] J. Xu, R.-C. Wu, B. W. O'Malley, *Nat. Rev. Cancer* **2009**, *9*, 615 – 630.
[4] C. A. Walsh, L. Qin, J. C. Tien, L. S. Young, J. Xu, *Int. J. Biol. Sci.* **2012**, *8*, 470 – 485.
[5] T. P. Yao, G. Ku, N. Zhou, R. Scully, D. M. Livingston, *Proc. Natl. Acad. Sci. USA* **1996**, *93*, 10626 – 10631.
[6] Y. Kamei, L. Xu, T. Heinzel, J. Torchia, R. Kurokawa, B. Gloss, S.-C. Lin, R. A. Heyman, D. W. Rose, C. K. Glass, M. G. Rosenfeld, *Cell* **1996**, *85*, 403 – 414.
[7] J. H. Kim, H. Li, M. R. Stallcup, *Mol. Cell* **2003**, *12*, 1537 – 1549.
[8] B. Belandia, R. L. Orford, H. C. Hurst, M. G. Parker, *EMBO J.* **2002**, *21*, 4094 – 4103.
[9] D. A. Rollins, M. Coppo, I. Rogatsky, *Mol. Endocrinol.* **2015**, *29*, 502 – 517.
[10] L. Qin, Z. Liu, H. Chen, J. Xu, *Cancer Res.* **2009**, *69*, 3819 – 3827.
[11] C. A. Walsh, L. Qin, J. C.-Y. Tien, L. S. Young, J. Xu, *Int. J. Biol. Sci.* **2012**, *8*, 470 – 485.
[12] D. M. Lonard, B. W. O'Malley, *Nat. Rev. Endocrinol.* **2012**, *8*, 598 – 604.
[13] D. M. Lonard, B. W. O'Malley, *Cell* **2006**, *125*, 411 – 414.
[14] X. Song, J. Chen, M. Zhao, C. Zhang, Y. Yu, D. M. Lonard, D.-C. Chow, T. Palzkill, J. Xu, B. W. O'Malley, J. Wang, *Proc. Natl. Acad. Sci. USA* **2016**, *113*, 4970 – 4975.
[15] Y. Wang, D. M. Lonard, Y. Yu, D.-C. Chow, T. G. Palzkill, B. W. O'Malley, *Mol. Endocrinol.* **2011**, *25*, 2041 – 2053.
[16] Y. Wang, D. M. Lonard, Y. Yu, D.-C. Chow, T. G. Palzkill, J. Wang, R. Qi, A. J. Matzuk, X. Song, F. Madoux, P. Hodder, P. Chase, P. R. Griffin, S. Zhou, L. Liao, J. Xu, B. W. O'Malley, *Cancer Res.* **2014**, *74*, 1506 – 1517.
[17] A. D. Rohira, F. Yan, L. Wang, J. Wang, S. Zhou, A. Lu, Y. Yu, J. Xu, D. M. Lonard, B. W. O'Malley, *Cancer Res.* **2017**, *77*, 4293 – 4304.
[18] Y. Zhao, Y. Yu, Y. Zhang, L. He, L. Qiu, J. Zhao, M. Liu, J. Zhang, *J. Steroid Biochem. Mol. Biol.* **2017**, *167*, 86 – 97.
[19] K. M. Sakamoto, K. B. Kim, A. Kumagai, F. Mercurio, C. M. Crews, R. J. Deshaies, *Proc. Natl. Acad. Sci. USA* **2001**, *98*, 8554 – 8559.
[20] D. P. Bondeson, A. Mares, I. E. D. Smith, E. Ko, S. Campos, A. H. Miah, K. E. Mulholland, N. Routly, D. L. Buckley, J. L. Gustafson, N. Zinn, P. Grandi, S. Shimamura, G. Bergamini, M. Faelth-Savitski, M. Bantscheff, C. Cox, D. A. Gordon, R. R. Willard, J. J. Flanagan, L. N. Casillas, B. J. Votta, W. den Besten, K. Famm, L. Kruidenier, P. S. Carter, J. D. Harling, I. Churcher, C. M. Crews, *Nat. Chem. Biol.* **2015**, *11*, 611 – 617.
[21] G. E. Winter, D. L. Buckley, J. Paulk, J. M. Roberts, A. Souza, S. Dhe-Paganon, J. E. Bradner, *Science* **2015**, *348*, 1376 – 1381.
[22] P. P. Chamberlain, L. G. Hamann, *Nat. Chem. Biol.* **2019**, *15*, 937 – 944.
[23] P. M. Cromm, C. M. Crews, *Cell Chem. Biol.* **2017**, *24*, 1181 – 1190.
[24] T.-T. Chu, N. Gao, Q.-Q. Li, P.-G. Chen, X.-F. Yang, Y.-X. Chen, Y.-F. Zhao, Y.-M. Li, *Cell Chem. Biol.* **2016**, *23*, 453 – 461.
[25] K. Raina, J. Lu, Y. Qian, M. Altieri, D. Gordon, A. M. K. Rossi, J. Wang, X. Chen, H. Dong, K. Siu, J. D. Winkler, A. P. Crew, C. M. Crews, K. G. Coleman, *Proc. Natl. Acad. Sci. USA* **2016**, *113*, 7124 – 7129.
[26] M. Schiedel, D. Herp, S. Hammelmann, S. Swyter, A. Lehotzky, D. Robaa, J. Oláh, J. Ovádi, W. Sippl, M. Jung, *J. Med. Chem.* **2018**, *61*, 482 – 491.
[27] B. Zhou, J. Hu, F. Xu, Z. Chen, L. Bai, E. Fernandez-Salas, M. Lin, L. Liu, C.-Y. Yang, Y. Zhao, D. McEachern, S. Przybranowski, B. Wen, D. Sun, S. Wang, *J. Med. Chem.* **2018**, *61*, 462 – 481.
[28] A. Zorba, C. Nguyen, Y. Xu, J. Starr, K. Borzilleri, J. Smith, H. Zhu, K. A. Farley, W. Ding, J. Schiemer, X. Feng, J. S. Chang, D. P. Uccello, J. A. Young, C. N. Garcia-Irrizary, L. Czabaniuk, B. Schuff, R. Oliver, J. Montgomery, M. M. Hayward, J. Coe, J. Chen, M. Niosi, S. Luthra, J. C. Shah, A. El-Kattan, X. Qiu, G. M. West, M. C. Noe, V. Shanmugasundaram, A. M. Gilbert, M. F. Brown, M. F. Calabrese, *Proc. Natl. Acad. Sci. USA* **2018**, *115*, 7285 – 7292.
[29] M. Brand, B. Jiang, S. Bauer, K. A. Donovan, Y. Liang, E. S. Wang, R. P. Nowak, J. C. Yuan, T. Zhang, N. Kwiatkowski, A. C. Müller, E. S. Fischer, N. S. Gray, G. E. Winter, *Cell Chem. Biol.* **2019**, *26*, 300 – 306.
[30] A. Varshavsky, *Proc. Natl. Acad. Sci. USA* **2019**, *116*, 358 – 366.
[31] A. Bachmair, D. Finley, A. Varshavsky, *Science* **1986**, *234*, 179 – 186.
[32] A. Varshavsky, *Proc. Natl. Acad. Sci. USA* **1996**, *93*, 12142 – 12149.
[33] C.-S. Hwang, A. Shemorry, D. Auerbach, A. Varshavsky, *Nat. Cell Biol.* **2010**, *12*, 1177 – 1185.

  

[34] S. M. Sriram, B. Y. Kim, Y. T. Kwon, *Nat. Rev. Mol. Cell Biol.* **2011**, *12*, 735 – 747.
[35] Y. T. Kwon, Y. Reiss, V. A. Fried, A. Hershko, J. K. Yoon, D. K. Gonda, P. Sangan, N. G. Copeland, N. A. Jenkins, A. Varshavsky, *Proc. Natl. Acad. Sci. USA* **1998**, *95*, 7898 – 7903.
[36] K. Shanmugasundaram, P. Shao, H. Chen, B. Campos, S. F. McHardy, T. Luo, H. Rao, *J. Biol. Chem.* **2019**, *294*, 15172 – 15175.
[37] Y. Lee, H. Yoon, S.-M. Hwang, M.-K. Shin, J. H. Lee, M. Oh, S.-H. Im, J. Song, H.-S. Lim, *J. Am. Chem. Soc.* **2017**, *139*, 16056 – 16059.
[38] J. Hou, U. Schindler, W. Henzel, T. Ho, M. Brasseur, S. McKnight, *Science* **1994**, *265*, 1701 – 1706.
[39] P. S. Foster, M. Martinez-Moczygemba, D. P. Huston, D. B. Corry, *Pharmacol. Ther.* **2002**, *94*, 253 – 264.
[40] J. S. Rawlings, K. M. Rosler, D. A. Harrison, *J. Cell Sci.* **2004**, *117*, 1281 – 1283.
[41] S. Goenka, M. H. Kaplan, *Immunol. Res.* **2011**, *50*, 87 – 96.
[42] K. Takeda, T. Tanaka, W. Shi, M. Matsumoto, M. Minami, S.-i. Kashiwamura, K. Nakanishi, N. Yoshida, T. Kishimoto, S. Akira, *Nature* **1996**, *380*, 627 – 630.
[43] C. M. Litterst, E. Pfitzner, *J. Biol. Chem.* **2001**, *276*, 45713 – 45721.
[44] C. M. Litterst, E. Pfitzner, *J. Biol. Chem.* **2002**, *277*, 36052 – 36060.
[45] W. S. Choi, B.-C. Jeong, Y. J. Joo, M.-R. Lee, J. Kim, M. J. Eck, H. K. Song, *Nat. Struct. Mol. Biol.* **2010**, *17*, 1175 – 1181.
[46] E. S. Fischer, K. Böhm, J. R. Lydeard, H. Yang, M. B. Stadler, S. Cavadini, J. Nagel, F. Serluca, V. Acker, G. M. Lingaraju, R. B. Tichkule, M. Schebesta, W. C. Forrester, M. Schirle, U. Hassiepen, J. Ottl, M. Hild, R. E. J. Beckwith, J. W. Harper, J. L. Jenkins, N. H. Thomä, *Nature* **2014**, *512*, 49 – 53.
[47] L. Qin, Y.-L. Wu, M. J. Toneff, D. Li, L. Liao, X. Gao, F. T. Bane, J. C.-Y. Tien, Y. Xu, Z. Feng, Z. Yang, Y. Xu, S. M. Theissen, Y. Li, L. Young, J. Xu, *Cancer Res.* **2014**, *74*, 3477 – 3488.
[48] L. Qin, X. Chen, Y. Wu, Z. Feng, T. He, L. Wang, L. Liao, J. Xu, *Cancer Res.* **2011**, *71*, 1742 – 1751.
[49] S. Wang, Y. Yuan, L. Liao, S.-Q. Kuang, J. C.-Y. Tien, B. W. O'Malley, J. Xu, *Proc. Natl. Acad. Sci. USA* **2009**, *106*, 151 – 156.
[50] X. Sun, H. Gao, Y. Yang, M. He, Y. Wu, Y. Song, Y. Tong, Y. Rao, *Signal Transduction Targeted Ther.* **2019**, *4*, 1 – 33.
[51] L. Zhang, B. Riley-Gillis, P. Vijay, Y. Shen, *Mol. Cancer Ther.* **2019**, *18*, 1302 – 1311.

Manuscript received: April 6, 2020
Revised manuscript received: June 1, 2020
Accepted manuscript online: July 6, 2020
Version of record online: August 12, 2020

  